Nuclear Inst. and Methods in Physics Research B 474 (2020) 1–5

Contents lists available at ScienceDirect

Nuclear Inst. and Methods in Physics Research B

journal homepage: www.elsevier.com/locate/nimb

Stripping of the NaI (Tl) detector response function for continuous energy photon spectrum by SVD approach

Ekrem Almaz[a,*], Ahmet Akyol[b]

[a] Muş Alparslan University, Science & Literature Faculty, Physics Department, Güzeltepe Kampus, 49250 Muş, Turkey
[b] Muş State Hospital, 49100 Muş, Turkey

ARTICLE INFO

Keywords:
Internal bremsstrahlung
Stripping
SVD Approach
Detector Response Function

ABSTRACT

We have tried to obtain the spectrum of internal bremsstrahlung photons which are released simultaneously with beta particles and neutrinos from the ^{90}Sr-^{90}Y source in secular equilibrium. Detector parameters of the 5.08 cm × 5.08 cm NaI(Tl) detector are determined using standard calibration sources. A detector response function is generated for a single-energy gamma photon using detector parameters and Monte Carlo method. The Singular Value Decomposition (SVD) method is used for stripping of the detector response function effects from the raw experimental spectrum. The stripped experimental data are compared with KUB theory and a different stripping method that we used our former work on the same isotope. There is a much better agreement between experimental and theoretical findings comparing the former experimental data.

1. Introduction

Internal bremsstrahlung (IB) spectrum is a weak, continuous electromagnetic radiation. The IB photon is emitted during the change in the dipole moment of the electron-nucleus couple system owing to the creation and separation of the electron and proton.

Total disintegration energy is shared between the IB photon, the beta particle, the neutrino and the recoil nucleus. IB should not be confused with external bremsstrahlung (EB) caused by loss of radiative energy with other particles rather than the nucleus from which the electron emerges [1].

First, Aston [2] experimentally demonstrated the existence of such an event. Knipp and Uhlenbeck [3], and independently, Bloch [4] at the same year developed the first theory using the Fermi polar vector interaction for allowed transitions of beta. Subsequent researchers tried to explain the IB event with new theoretical approaches for allowed and forbidden transition, including the Coulomb and detour transition effect [5–9]. In this study, we have stripped or unfolded the effects of detector response function (DRF) by SVD method from the experimental data. Stripping procedure of IB spectrum with the approach of SVD method was first discussed by in our study on the IB spectrum of the ^{204}Tl isotope [10]. The study has shown that this method can be used effectively in stripping the raw spectrum from the effects of detector response function. In this experimental setup, another beta emitter ^{90}Sr-^{90}Y in secular equilibrium was used as source of IB. Through this work, we have had the opportunity to compare the IB results of SVD method with the ones obtained from Gold iteration method of our previous work [11] for the same isotope.

We also compared the stripped data with KUB theory results. One can find detailed information about having IB spectra by KUB theory as well as Monte Carlo Method in the studies of Almaz and Cengiz [12] and Cengiz and Almaz [13].

2. Experiment

^{90}Sr has a first forbidden transition and disintegrates into the ^{90}Y radioisotope by releasing beta particles with endpoint energy of 546 keV. ^{90}Y is a single first forbidden source of beta and has two branches which decay to ^{90}Zr isotope. The first branch emits a beta particle with an endpoint energy of E_m = 2277.4 keV and has a 99.98% probability of disintegration. The second branch emits beta with an endpoint energy of E_m = 513 keV and has a 0.02% emitting probability [14]. The actual IB photon spectrum is blurred by the detector response function which means the response function effects are imposed on the spectrum. In addition, the spectrum is highly affected by statistical fluctuations. In order to have the true IB spectrum, the spectrum obtained from the detector must be stripped from the response effects.

Using singular value decomposition technique, the effects of detector response function were unfolded from the measured experimental spectrum as well as the statistical fluctuations were kept to a minimum. In the

* Corresponding author.
E-mail address: e.almaz@alparslan.edu.tr (E. Almaz).

https://doi.org/10.1016/j.nimb.2020.04.019
Received 15 January 2020; Received in revised form 6 March 2020; Accepted 17 April 2020
Available online 23 April 2020
0168-583X/

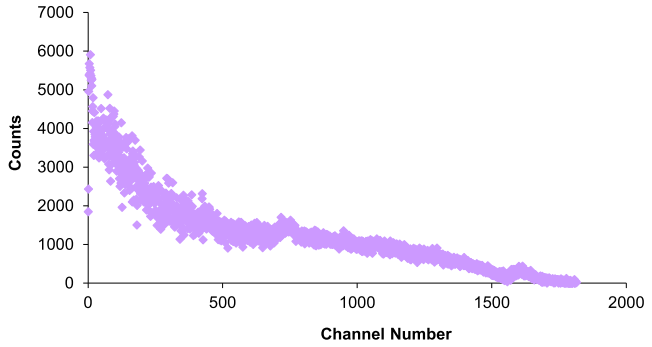

Fig. 1. Background corrected experimental photon spectrum from the ^{90}Sr-^{90}Y beta source counted in NaI (Tl) detector system. Calibration of the detector and detector response functions of NaI(Tl) detector were determined using standard gamma source isotopes ^{241}Am, ^{137}Cs, ^{22}Na and ^{60}Co.

initial stage of the experiment, the magnetic deflection method, which is one of the several methods used in IB experiments, was engaged to prevent the beta from the source to enter the detector and release the EB. With this setup, the possibility of external bremsstrahlung was kept to a minimum by deflecting the beta particles and impinging them on low Z material. Commercial NaI (Tl) detector of 5.08 cm × 5.08 cm was used in the experiment. The typical resolution (FWHM) value of this detector is about 7–8% for the 661.6 keV gamma of ^{137}Cs.

5.08 cm × 5.08 cm NaI(Tl) scintillation crystal coupled directly to a photomultiplier tube with a rigid, high refractive index, optical coupling medium. The crystal and the matching photomultiplier tube were hermetically sealed in a low mass light-tight housing having an aluminum entrance window. The housing consists of a thin aluminum can around the crystal connected to a mu-metal shield which surrounds the photomultiplier tube. Data from the detector were recorded on the Canberra 40 series MCA with appropriate amplifications and taken from a 2047 channel spectrometer. In the same counting period, the natural background was counted and subtracted from the raw spectrum. The experimental spectrum obtained is given in Fig. 1. The maximum energy taken from the spectrometer of the IB photons of the β^- particles with endpoint energy of 2277.4 keV, as seen in Fig. 1 could be measured up to the 1800th channel which means up to 1710 keV according to our calibration. Therefore, IB photons emitted in energy greater than this energy have been neglected. Since the statistical fluctuations are high as shown in Fig. 1, the channel width is increased to 1710 keV / 45 = 38 keV to smooth the spectrum and enable the spectrum stripping process. This spectrum has been redrawn in Fig. 5 along with the response function spectrum with a channel width of 38 keV.

Peak to total ratio (P/T), total and full energy peak efficiencies and energy resolution of the detector were obtained for the DRFs. Depending on the energy of the incoming gamma ray, the detector parameters were fitted to the optimal values using the fit functions. The functions and fit parameters with energy values in keV unit are given in Table 1.

The fit functions obtained are valid in the 10 keV ≤ E ≤ 1400 keV energy region. Since the experimental deviations are high in full energy peak and total efficiency values in the energy region less than 60 keV, deviations in fit functions are also high in this region. Therefore there is a mismatch between functions such as $E_p > E_t$. In the experiment with 5.08 cm × 5.08 NaI (Tl) detector, full energy peak efficiency, E_p function is used and the total efficiency, E_t, function is not chosen for the reason given above. So, we prefer to use P/T polynomial function for defining the peak to total ratio. Since the P/T function takes values greater than 1 in the region of E < 24 keV, P/T ratios are taken as 1.

3. Spectral stripping and data analysis

The ^{90}Sr radioactive source having an activity of 10 μCi was counted on the detector for more than 100 h until having a sufficient statistical data. The pulse-height distribution obtained in the detector and the photon distribution to the detector will be completely different considering all energy values. No matter how good your detector is, the measured experimental spectrum and the energy spectrum of the incoming photon will not be the same. However, true spectrum measurements, especially in dosimetry, are of great importance in the measurement of air-kerma ratios for γ and x-rays, and the stopping power of γ-rays. In radiation detection, the Gaussian distribution (in relation to the detector resolution function) is actually folded into the measured spectrum. If we want to express that mathematically, folded spectrum (pulse height spectrum obtained from experiment) *M (E′)* can be written in the form,

$$M(E') = \int_0^\infty R(E', E) S(E)\, dE. \tag{1}$$

Here *S (E)* is the incoming spectrum of photon and *R (E′, E)* is the detector response function. This function is actually the first order Fredholm integral which is frequently encountered in engineering and basic sciences [15]. This integral can be expressed in discrete matrix form:

$$\begin{bmatrix} M_1 \\ \vdots \\ M_m \end{bmatrix} = \begin{bmatrix} R_{11} & R_{12} & \cdots & R_{1n} \\ \vdots & \vdots & \ddots & \vdots \\ R_{m1} & R_{m2} & \cdots & R_{mn} \end{bmatrix} \begin{bmatrix} S_1 \\ \vdots \\ S_n \end{bmatrix} \Rightarrow M = R\,S. \tag{2}$$

Here, the probability R_{ij} is the probability that an incident gamma ray energy falling into the energy bin *i*, is counted in the bin *j*. The main task here is to extract the incoming photon spectrum from the measured spectrum using the most appropriate stripping method.

3.1. Obtaining DRFs

The photons counted in the photopeak region of the response function can be obtained by

$$N_P = \varepsilon_P N_y. \tag{3}$$

Here ε_p is the full energy peak efficiency given in Table 1. N_p and N_y are the photons counted in photopeak region and photons emitted from the source respectively. The number of photons counted in Compton region can be calculated from the expression,

$$N_C = N_P\left(\frac{1}{\varepsilon_{PT}} - 1\right). \tag{4}$$

where ε_{PT} is the peak to total ratio and can be expressed as,

$$\varepsilon_{PT} = \frac{N_P}{N_S}. \tag{5}$$

where N_s is defined as the number of photons counted in the detector and formulated as $N_s = N_c + N_p$. Once the N_p and N_c values were determined, the detector response functions were normalized to 1 by dividing the number of photons emitted from the source

which is taken as a constant $N_y = 10^7$ for each calculated photon energy. Thus, the numbers obtained in response functions gives the counting probability on the relevant channel of a photon emitted from the source. The Compton edge corresponding to E_j energy is calculated from,

$$E_C = E_j \frac{2E_j/mc^2}{1 + 2E_j/mc^2}. \tag{6}$$

The N_c photons falling in the Compton region are shared equally to the channels whose width is ΔE_j. The photons falling on the photopeak region and the channels in the Compton region were distributed to the Gaussian function with a standard deviation σ_j by Gauss distribution sampling. If the energy left by the photon to the detector is E_j, Gauss distribution which gives the pulse height distribution of the photon due to the detector resolution is,

Table 1
The functions and the fit parameters for the energy resolution, full energy peak and total efficiencies and peak to total ratio values for the 5.08 cm × 5.08 cm NaI (Tl) detector.

Function Name and Expression	Parameters				
	p_1	p_2	p_3	p_4	p_5
Energy Resolution (%): $R = \frac{\Delta E}{E} = (p_1 e^{p_2 E} + p_3 E^{p_4})$	264.36	−0.063791	102.65	−0.4089	–
Full Energy Peak Efficiency (%)*: $\varepsilon_P = p_1 e^{-\frac{(x-p_2)^2}{2p_3{}^2}} + p_4 + p_5 x$	54.4431	−0.6122	6.3579	−59.5702	4.7409
Total Efficiency (%)*: $\varepsilon_t = p_1 e^{-\frac{(x-p_2)^2}{2p_3{}^2}} + p_4 + p_5 x$	125.1604	−2.9050	8.9923	−124.2825	8.1094
Peak/Total Ratio (P/T)*: $\varepsilon_{PT} = 1 + p_1 x + p_2 x^2 + p_3 x^3 + p_4 x^4$	0.083399	−0.028217	$7.4{\cdot}10^{-4}$	$-6.9{\cdot}10^{-5}$	–

* $x = \ln E\,(keV)$.

$$P_G(E_P) = \frac{1}{\sigma_j \sqrt{2\pi}} \exp\left(-\frac{(E_P - E_j)^2}{2\,\sigma_j{}^2}\right). \tag{7}$$

where E_p is the detected photon energy as a puls height. The standard deviation depending on the resolution function is calculated from,

$$\sigma_j = E_j \frac{R}{2.35482}. \tag{8}$$

where E_j is the photon energy and R is the energy resolution function given in Table 1.

Rejection Method was used in sampling of Gauss distribution with Monte Carlo Method. Each of the Gauss Distributions is sampled in the range of -3σ *to* $+3\sigma$ which covers 99.7% of the distribution. The basic Monte Carlo principle has been applied to the rectangular (uniform distribution) rejection function as,

$$q = \frac{\int_{E_{\min}}^{E} dE}{\int_{-3\sigma}^{3\sigma} dE} = \frac{E - E_{\min}}{E_{\max} - E_{\min}} = \frac{E - E_{\min}}{6\,\sigma}, \tag{9}$$

and that gives,

$$E = E_{\min} + q \cdot 6\,\sigma. \tag{10}$$

where q is a random number with uniform distribution in the range of 0 to 1, $E_{min} = E_j - 3\sigma_j$ and $E_{max} = E_j + 3\sigma_j$, $(j = 1,2,3, \ldots, n, n+1)$. Here $E = E_1, E_2, E_3, \ldots, E_n$ are the energy values of the Compton region divided into n-pieces of energy regions and $E_{n+1} = E$ is the energy value of the gamma corresponding to the photopeak emitted from the source. The midpoint of each energy region was chosen as the energy value. By generating a random number q, E_p value was obtained from the Eq. (10). Generating a second random number q, the condition was checked as,

$$q < e^{-(E_p - Ej)^2/2\sigma_j{}^2}. \tag{11}$$

If the condition is fulfilled, this E_p value is counted in the relevant sub energy region, if the condition is not met, the process is repeated [16]. Thus, the response function of an E energy of gamma source is obtained. Fig. 2 shows how DRFs are obtained graphically. Each bin is contributed by Gaussian distribution due to the detector resolution from adjacent bins.

3.2. Singular value decomposition (SVD)

The SVD method has become a widely used calculation tool in statistical data analyses, signal processing, system identification, control system analysis and including spectral estimation. The object of studying the SVD of a matrix is to build approximations of the full $m \times n$ matrix by only using a number of the terms of the diagonal matrix in the decomposition process. This approximation of the full matrix is the basis of response compression. Using SVD, the $m \times n$-sized

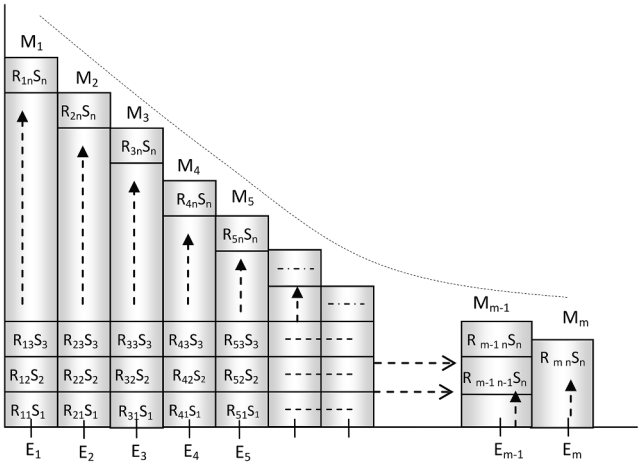

Fig. 2. Displaying of counts in each channel of the photon spectrum measured in the detector [17].

response matrix compressed in DRFs can thus be unfolded, since the counts in each bin of the detector system form a matrix element in the response matrix. The key here is to determine the singular values (Σ). Singular values follow a decreasing sequence. The first singular value is larger and the subsequent ones are in decreasing order.

R is a real and $m \times n$-sized matrix, SVD is the factorization of this matrix form of $R = U\,\Sigma\,V^T$, where U, $m \times m$ size orthogonal matrix $(U\,U^T = U^T\,U = I)$, V represents $n \times n$ dimensional orthogonal matrix $(V\,V^T = V^T\,V = I)$ and Σ represents $m \times n$ non-negative diagonal matrix. Σ_{ij} elements can be expressed as $\Sigma_{ij} = 0$ for $i \neq j$ and $\Sigma_{ii} \equiv \sigma_i \geq 0$. Here, the σ_i numbers are called singular values of matrix R. The singular values contain valuable information about the properties of a matrix. For example, if R itself is orthogonal, all singular values of σ_i are equal to 1, if R is degenerated; at least one singular value of σ_i becomes equal to zero [18–21]. Fig. 3 illustrates the SVD process visually.

In fact, the rank of a matrix is the number of individual non-zero values. If the right side of the matrix and /or equation of a linear system are known with a certain level of uncertainty, and some singular values of the matrix are significantly smaller than others, the system may be difficult to solve even if the matrix is fully ordered. In many ways, such matrices behave like degenerate ones, and SVD proposes a method to solve such problems which are common to small and completely zero singular values. We assume that the individual values σ_i form a non-incrementing frequency sequence. The decomposition of an R matrix contains the diagonal Σ matrix of size $m \times n$ and can be written in the form of a matrix:

$$\Sigma = \begin{bmatrix} D & 0 \\ 0 & 0 \end{bmatrix}_{\leftarrow \text{m−r rows}} \quad \uparrow \text{n − r columns} \tag{3}$$

Here, D is a diagonal $r \times r$ size matrix for r values not exceeding the

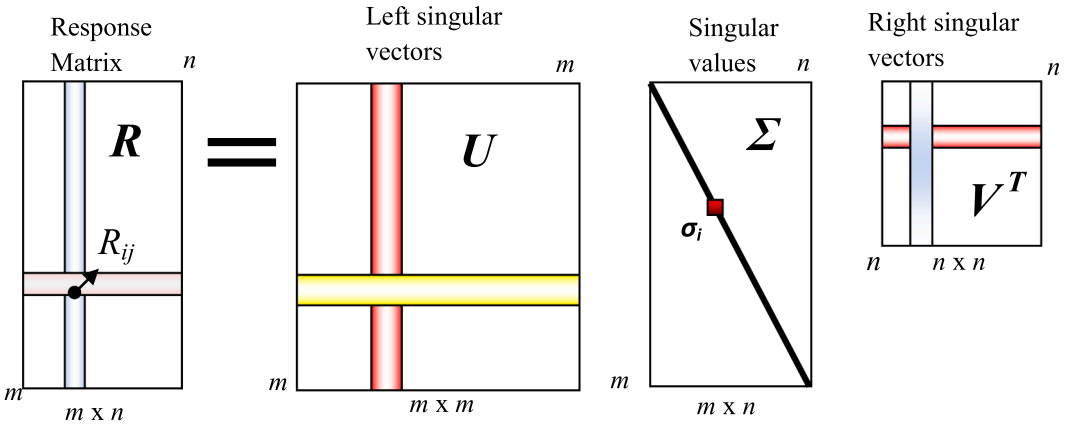

Fig. 3. Visualization of the matrix multiplications in singular value decomposition.

smaller ones of m and n (if r is equal to m or n or both, some or all of the zero matrices are not visible) [19].

Comprehensive explanations and many technical details and examples of SVD can be found in literature [22,23]. Indeed, one of the most attractive features of this process is that you do not have to calculate SVD manually. In addition, we have used the SVD subroutine that exists under the Matlab™ program. Accordingly, we created the experimentally obtained values in the form of column matrix. By using Monte Carlo method and detector parameters, as described above, the detector response in the form of a matrix of $m \times n$ size was created. The matrices which are generated were entered into Matlab program as txt –ascii code and consequently SVD method was applied. When the matrix is decomposed into the form of $R = U\,\Sigma\,V^T$, its properties can be easily analyzed and very easy to manipulate. Such an analysis is very useful for poorly defined linear systems with almost (or even fully) degenerate matrices, because it not only identifies the difficulty, but can also suggest ways to overcome it. If we try to solve the problem directly from the inverse solution without using approaches like SVD or the Gold iteration method that we have used before, the direct inverse solution of the response matrix , namely the inverse solution of $S = R^{-1}M$, brought undesirable negative solutions in the solution vector S as in Fig. 4. The reason for this situation is thought to be due to the very large reflection of small statistical deviations in the response matrix to the result in the high energy region. As predicted in the literature [24], negative values were obtained after certain energy. Since the detector response matrix is high-dimensional and the IB photon energy is divided into certain energy ranges (channels), there are negative physical results from the inverse solution due to statistical fluctuations between neighboring channels. Therefore, we need different methods for approaching to strip the effects of the detector response function. No matter how good the response matrix you are setting up, even a small fluctuation between channels is greatly reflected in the resulting stripped spectrum. Compared with the Gold Iteration method [11] that we applied earlier, better results were obtained in the IB spectrum for the ^{90}Sr-^{90}Y isotope by SVD method.

4. Results and discussion

Fig. 5 shows the raw detector spectrum of the ^{90}Sr with the background correction. This spectrum forms the *M (E)* values used in the Eq. (2) and the spectrum values taken as the sum of the values of the column of the response matrix obtained in 45 × 48 matrix dimensions.

We solved the SVD problem for DRFs by writing code in Matlab™. As can be seen in Fig. 6, when the data obtained is plotted, it is observed that the SVD solution fits very well with the KUB theory values up to the experimental energy limit of 1400 keV for DRFs. Furthermore, the unfolded experimental values gathered by Gold Iteration Method from our former study are also shown in the graph [11].

In IB studies with almost all forbidden beta transitions, a positive deviation in the high energy region is observed between experimental data and theoretical values [25–28]. As a result of the experiment performed in this study, statistically robust data could be obtained up to

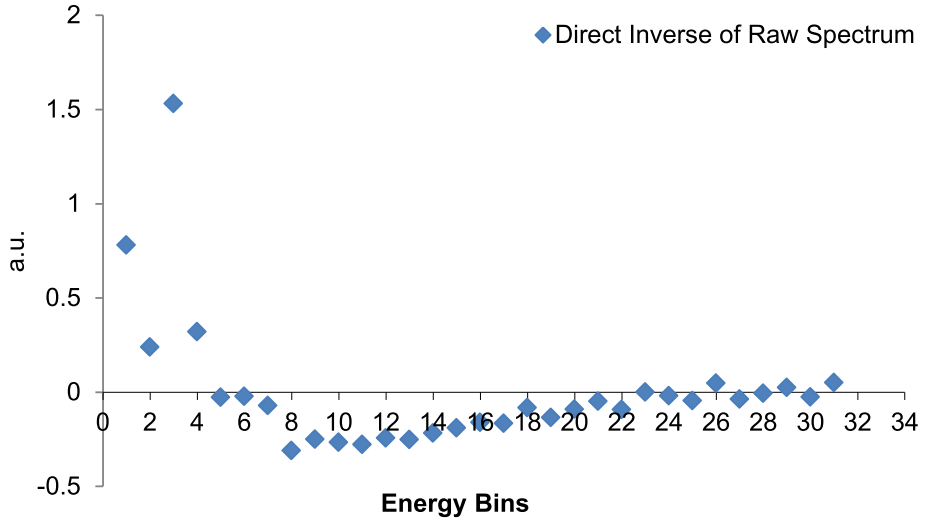

Fig. 4. Result spectrum with negative values obtained by taking the direct inverse of the response matrix.

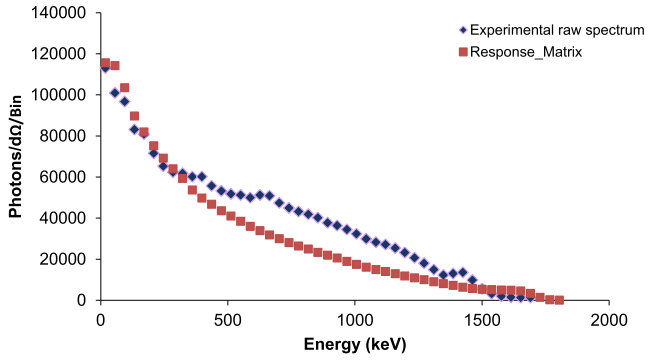

Fig. 5. Experimental background corrected photon spectrum of ^{90}Sr-^{90}Y isotope obtained by taking the channel width 38 keV and detector response matrix normalized to the experimental values.

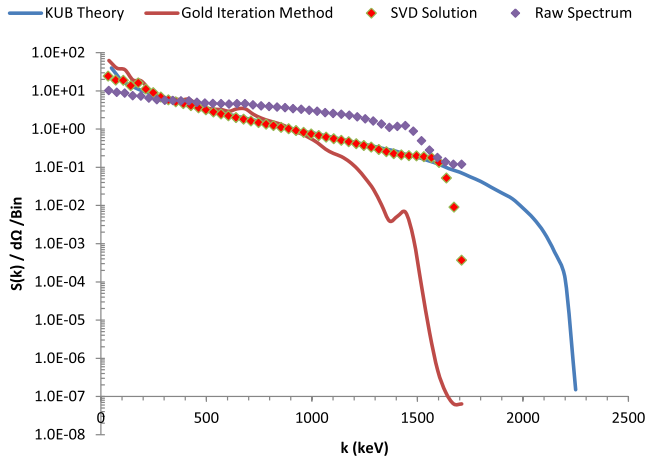

Fig. 6. Comparisons of the spectra in a semi-log plot: Applying the SVD method to experimental spectrum, KUB theory result, Gold iteration method from the former study and the raw energy spectrum. All spectra are normalized according to raw spectrum and showed as photons per steradian per energy bin versus energy.

1400 keV in the energy limit of the experiment with NaI (Tl) detector, although SVD approximation values are compatible with experimental values up to 1700 keV energy limit. Statistically accurate data were not observed in the channels after this energy. There are several reasons behind the deviations in the high energy region. First, failure to establish the detector response matrix accurately can cause deviation from the actual IB spectrum after stripping. Nuclear virtual gamma transitions (detour transitions) show an increase in the spectrum overlying the internal bremsstrahlung spectrum [7]. Another factor is the limitation of counting statistics due to the low probability of IB as it approaches the end of the energy spectrum. This creates a fluctuation on the actual data. However, when the Fig. 6 is examined, the experimental results stripped by the SVD method show a very good agreement with KUB theory between 50 keV and 1400 keV. It is easily seen that this result is better than our former study [11] in which Gold iteration method is applied for the stripping process for the same radioisotope. Here it is possible to draw the following result: Gold iteration method is much more affected by statistical fluctuations than SVD method, which corresponds to the deviations from the theoretical values in the stripped spectrum as shown in Fig. 6. In the SVD method, statistical deviations were observed much less, which means that the method is more stable at each energy value. In addition, it is concluded that the detector parameters of the response matrix are determined very well and the detector response function generated for each energy value of the gamma obtained by Monte Carlo method along with the detector parameters is applied in a very good simulation.

CRediT authorship contribution statement

Ekrem Almaz: Conceptualization, Formal analysis, Methodology, Software, Supervision, Validation, Writing - original draft, Writing - review & editing. **Ahmet Akyol:** Investigation, Visualization, Resources, Data curation.

Declaration of Competing Interest

The authors declare that they have no known competing financial interests or personal relationships that could have appeared to influence the work reported in this paper.

References

[1] B.G. Pettersson, Alpha, beta and gamma ray spectroscopy, Vol-2, (Edt: Kai Siegbahn), North-Holland Publishing Company, Amsterdam, 1965.
[2] G.H. Aston, Proc. Camb. Philos. Soc. 23 (1927) 935–941.
[3] J.K. Knipp, G.E. Uhlenbeck, Physica 3 (1936) 425–439.
[4] F. Bloch, Phys. Rev. 50–1 (1936) 272–279.
[5] P.R. Lewis, G.W. Ford, Phys. Rev. 107–3 (1957) 756–765.
[6] L. Spruch, W. Gold, Phys. Rev. 113 (1959) 1060–1069.
[7] G.W. Ford, C.F. Martin, Nucl. Phys. A 134 (1969) 457–469.
[8] C.S.W. Chang, D.L. Falkoff, Phys. Rev. 76 (1949) 365–372.
[9] P. Bolgiano, L. Madansky, F. Rasetti, Phys. Rev. 89 (1953) 679–684.
[10] E. Almaz, Appl. Radiat. Isot. 99 (2015) 35–40.
[11] E. Almaz, A. Cengiz, A. Tartar, Int. J. Mod. Phys. E 16 (2007) 1733–1740.
[12] E. Almaz, A. Cengiz, X-ray Spectrom. 36 (2007) 419–423.
[13] A. Cengiz, E. Almaz, Radiat. Phys. Chem. 70 (2004) 661–668.
[14] C.M. Lederer, V.S. Shirley, Table of Isotopes, 7th ed., Wiley, New York, 1978.
[15] A.N. Tikhonov, A.V. Goncharsky, V.V. Stepanov, A.G. Yagola, Numerical Methods for the Solution of Ill-posed Problems, Kluwer Academic Publishers, The Netherlands, 1995.
[16] Reuven Y. Rubinstein, Dirk P. Krouse, Simulation and The Monte Carlo Method, second ed., Wiley Interscience, New Jersey, 2008.
[17] E. Almaz, The Analysis of Internal Bremsstrahlung Spectra of Beta Particles (Ph.D. thesis), Uludağ University, Bursa, Turkey, 2007.
[18] M. Moonen, B. De Moor, SVD and Signal Processing, III: Algorithms, Architectures and Applications, Elsevier Publishing, The Netherlands, 1995.
[19] D.C. Lay, Linear Algebra and Its Applications, fourth ed. Pearson, Addison-Wesley Publishing Company, Boston, 2012.
[20] W.H. Press, S.A. Teukolsky, W.T. Vetterling, B.P. Flannery, Numerical Recipes the Art of Scientific Computing, third ed., Cambridge University Press, NewYork, 2007.
[21] H. Yanai, K. Takeuchi, Y. Takane, Projection Matrices, Generalized Inverse Matrices and Singular Value Decomposition, Springer-Verlag, New York, 2011.
[22] C.E. Lawson, R.J. Hanson, Solving Least Square Problems, Prentice-Hall Inc., Englewood Cliffs, 1974.
[23] G.E. Forsythe, M.A. Malcolm, C.B. Moler, Computer Methods for Mathematical Computations, Prentice-Hall Inc., Englewood Cliffs, 1977.
[24] G. Cowan, Statistical Data Analysis, Clarendon Press, Oxford, 1998.
[25] B.R.S. Babu, P. Venkataramaiah, K. Gopala, H. Sanjeeviah, J. Phys. G: Nucl. Phys. 11 (1999) 1213–1220.
[26] B.R.S. Babu, A. Basaravaju, P. Venkataramaiah, K. Gopala, H. Sanjeeviah, Phys. Rev. C 32 (1985) 1010–1013.
[27] P. Venkataramaiah, H. Sanjeeviah, B. Sanjeevaiah, J. Phys. G: Nucl. Phys. 6 (1980) (1980) 1443–1451.
[28] K.S.G. Rao, P. Venkataramaiah, K. Gopala, H. Sanjeeviah, Nucl. Phys. A 365 (1981) 1–7.